Available online at www.sciencedirect.com
SCIENCE DIRECT®
Wear 257 (2004) 696–707
WEAR
www.elsevier.com/locate/wear

Mechanical and tribological properties of PA/PPS blends☆

Zhaobin Chen[1], Tongsheng Li*, Yuliang Yang, Xujun Liu, Renguo Lv

Department of Macromolecular Science, Key Laboratory of Molecular Engineering of Polymers, MEC, Fudan University, Shanghai 200433, PR China

Received 16 June 2003; received in revised form 16 March 2004; accepted 16 March 2004

Abstract

Polymer blending is a very important and widely used method for the modification of polymer materials. The mechanical properties, miscibility and modification mechanisms of blends have been investigated earlier. However, studies of their tribological behavior have been few, and little attention has been paid to the friction and wear mechanisms of polymer blends. In this paper, the structure, mechanical and tribological properties of polyamide 66 (PA66) and polyphenylene sulfide (PPS) blends were studied. It was found that the PA66/PPS blends had a two-phase structure; the blend with 30 vol.% PPS exhibited the best general mechanical properties; 80 vol.% PA66–20 vol.% PPS blend had the lowest wear.

Differential scanning calorimetry (DSC) and Fourier transform infrared spectrometry (FT-IR) analyses were carried out and the transfer films on the mating steel surfaces were investigated by scanning electron microscopy (SEM) and energy dispersive spectrometer (EDS). The results indicated that the crystalline structure of PA66, PPS and PA66/PPS blends changed due to sliding and tribochemical reactions occurred with the PA66 and the PA66 phases in blends. The thermal control of friction model is applicable to this blend system, i.e. the friction coefficient of PA66/PPS blends depended on the PA66 component with lower melting point, while the wear properties were governed by the adhesive ability between the PPS and the counterface.

Keywords: PA/PPS blends; Tribology; Transfer film; FT-IR; Thermal control of friction

1. Introduction

The use of polymers and polymer-based composites is very common in situations where a combination of good mechanical and tribological properties is required. It is often found that such properties are not attainable with a homopolymer. The methods of polymer modification include copolymerizing, reinforcing and blending. Polymer blending is fascinating because it has simple processing and unfolds unlimited possibilities of producing materials with variable properties. These advantages have led to its rapid use in applications of polymers. In the field of polymer tribology, in addition to adding internal lubricants (PTFE, silicon oil, etc.) and anti-wear fillers (inorganic powders, fibers, etc.), blending is also a traditional and effective way [1–4].

Polyamide (PA) is a widely used engineering plastic. It possesses an outstanding combination of properties such as low density, easy processing, good strength and solvent resistance. However, its heat distortion temperature is low and because of the presence of amide groups in the molecular chain, it easily absorbs water which deteriorates its mechanical properties and dimensional stability. Polyphenylene sulfide (PPS) possesses high temperature resistance combined with good mechanical properties, exceptional chemical and solvent resistance, high dimensional stability and easy processing. It has, however, a lower elongation to break, a higher cost and is rather brittle. In order to improve these adverse effects, some researchers have blended both materials and obtained a polymer alloy with outstanding properties [5–7]. However, these studies were focused on the melting stability, structural uniformity and mechanical properties of PA/PPS blends, but not on their friction and wear properties.

Studies of the tribological properties of PA, PPS and their composites have been reported in previous literature [8–19]. The superior wear resistance of PA compared with other polymers has been attributed to its ability to form an adhesive transfer film when sliding against metal counterface. PPS has high friction coefficient and wear because it does not form a strong transfer film on a metal counterface. In the present

☆ The Key Scientific and Technological Project, Ministry of Education, PR China.
* Corresponding author. Tel.: +86-21-50801330-126; fax: +86-21-50801711.
E-mail address: lits@fudan.edu.cn (T. Li).
[1] Present address: Department of Human Ecology, University of Texas at Austin, TX 78712, USA. E-mail: 000542@fudan.edu.cn (Z. Chen).

0043-1648/$ – see front matter © 2004 Elsevier B.V. All rights reserved.
doi:10.1016/j.wear.2004.03.013

Table 1
Materials used in this study

Polymer	Supplier	Trade name	Melting point (°C)	Specific gravity (g/cm^3)
PA66	DuPont Co. Ltd.	Zytel 101L NC010	262	1.14
PPS	Chevron Phillips Chemical Co.	Ryton P-4	285	1.35

work, which investigates the structure and the mechanical properties of PA66/PPS blends, the authors emphasize the tribological properties of the polymer blends. The friction and wear mechanisms are discussed in terms of the structure and transfer films.

2. Experimental details

2.1. Materials

PA66 in granular form and PPS in powder form were used in this paper and the data on these materials are given in Table 1.

2.2. Specimen preparation

PA66/PPS blends were prepared in the following volume ratios: 100/0, 80/20, 70/30, 60/40, 30/70 and 0/100, using a HAAKE PTW16/25D co-rotating twin-screw extruder. Following Refs. [5–7], the temperatures from the feed zone to the die of the extruder were 265, 275, 285, 295 and 285 °C, respectively. The diameter of the die is 3 mm. The screw speed was set at 70 rpm. All the materials were dried at 100 °C for 24 h before compounding. The extrudate was obtained in the form of a cylindrical rod that was quenched in cold water and then pelletized.

The specimens for mechanical and tribological tests were injection molded from the pelletized blend materials using a SZ-20 reciprocating screw injection-molding machine equipped with a standard test mould. The temperatures maintained in the two zones of the barrel were 280 and 300 °C, and in the mould 25 °C.

2.3. Measurements of material properties

The thermal analysis was conducted on a NETZSCH DSC204 at a heating rate of 10 K/min. The structure of the materials was examined with a Nicolet NEXUS470 FT-IR transmission mode. The morphologies of the polymer blends were characterized with a JSM-5600LV SEM. The blends were fractured in liquid nitrogen, then the fracture surfaces were etched with *m*-cresol to remove the PA66. The samples were sputter-coated with a gold palladium alloy prior to viewing under the microscope.

The tests of tensile strength, flexural strength, impact strength and Rockwell hardness (HRM) were conducted according to GB/T 16421-1996, GB/T 16419-1996, GB/T 16420-1996 and GB/T 9342-88, respectively.

The friction and wear tests were conducted on an M-200 friction and wear tester. A schematic diagram of the frictional pairs is shown in Fig. 1. A carbon structure steel ring (No. 45, GB 699-88) of 40 mm outer diameter was used as the counterface. The polymer specimen blocks were 6 mm × 7 mm × 30 mm. Before each test, the surfaces were polished with metallographic abrasive paper to R_a 0.17–0.23 μm for the specimens and R_a 0.09–0.11 μm for the counterfaces. Then the blocks and the rings were ultrasonically cleaned in acetone and thoroughly dried. Sliding was performed under ambient conditions (temperature: 20 ± 5 °C, humidity: 50±10%) at a speed of 0.42 m/s and a normal load of 196 N. The test durations ranged from 0 to 130 min and the values of friction torque were noted after 10 min and later at intervals of 20 min. The transient friction coefficient was calculated from the friction torque. The average values of friction

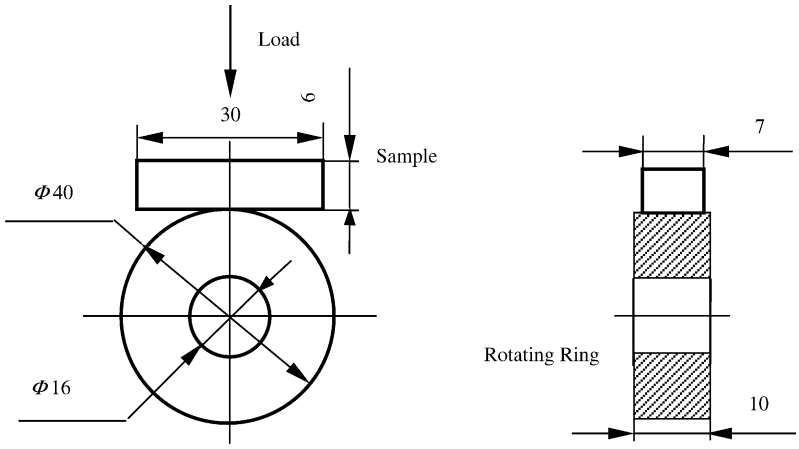

Fig. 1. Contact schematic diagram for the frictional couple (mm).

coefficient in the steady state were used as the friction coefficient of samples. At the end of each test, the width of the wear scar was measured with a measuring microscope, and the wear volume V of the specimen was calculated from the relationship [20]:

$$V = B\left[\frac{\pi r^2}{180}\arcsin\left(\frac{b}{2r}\right) - \frac{b}{2}\sqrt{r^2 - \frac{b^2}{4}}\right]$$

where V is the wear volume loss (mm^3), B the width of the specimen (mm), r the radius of the steel ring (mm) and b the width of the wear scar (mm). In this work, three replicate friction and wear tests were carried out.

2.4. Surface analysis

The transfer films formed by the specimens were examined by SEM. The elemental compositions in the transfer films were investigated by Oxford Instrument 6587 EDS. Wear debris were analyzed by DSC and FT-IR to understand the physical and chemical changes during sliding.

3. Results and discussion

3.1. Blend structure

The DSC curves of PA66, PPS and their blends are shown in Fig. 2. It can be seen that all the blends show two melting peaks at 265 and 286 °C which correspond to the melting points of PA66 and PPS, respectively. This indicates that the polymer blends are immiscible on a molecular scale and have a two-phase structure.

The enthalpies of the PA66 and PPS phases in the blends as calculated from Fig. 2 are listed in Table 2. From the data in this table, it can be seen that the enthalpies of PA66 and PPS phases in the blends are lower than that of the pure polymers and decrease with the decrease in their respective contents. This indicates that in the blending process, the crystalline regions in PA66 and PPS are arranged irregularly and the crystallinity decreases.

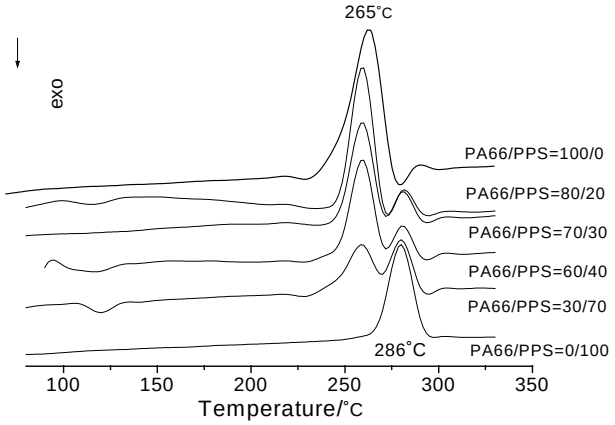

Fig. 2. The DSC traces of PA66, PPS and PA66/PPS blends.

Table 2
The enthalpies (ΔH, J/g) of the PA66 and PPS phases in the blends

	100/0	80/20	70/30	60/40	30/70	0/100
PA	67.6	56.71	47.99	37.41	16.65	–
PPS	–	5.8	8.2	9.5	20.5	59.8

The FT-IR spectra of PA66, PPS and a PA66/PPS (70/30) blend are shown in Fig. 3. The characteristic absorption bands of PA66 are: stretching vibration of C=O at 1636 cm^{-1}, deformation vibration of N–H at 1539 cm^{-1}, stretching vibration of C–N at 1270 cm^{-1} and bending

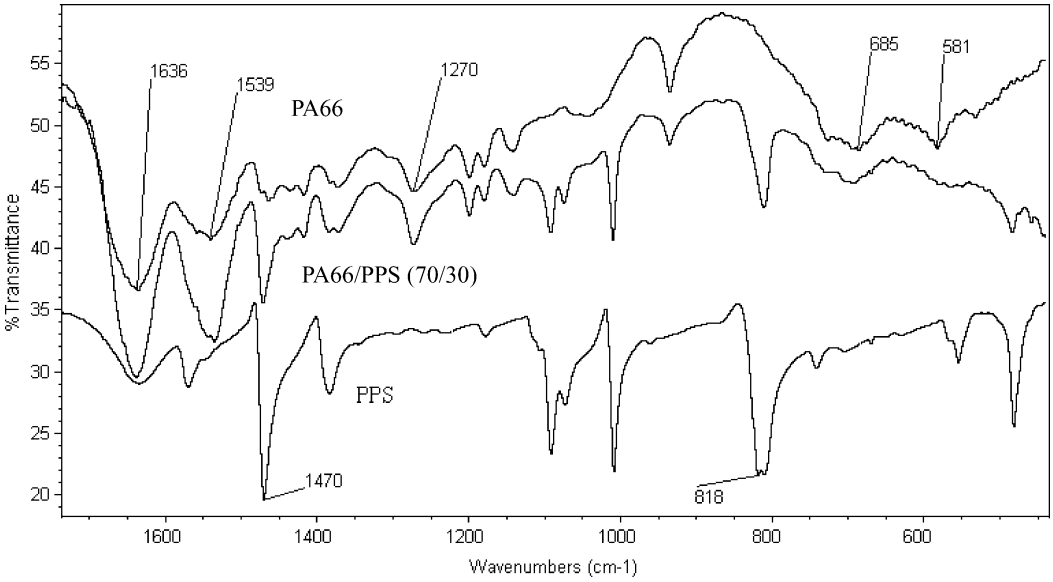

Fig. 3. FT-IR spectra of PA66, PPS and a PA66/PPS (70/30) blend.

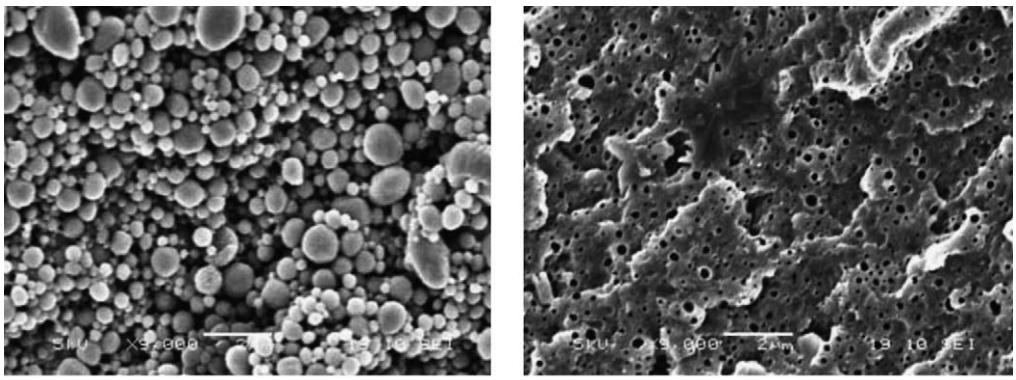

(a) PA66/PPS (80/20). (b) PA66/PPS (30/70).

Fig. 4. SEM micrographs of PA66/PPS blends.

vibrations of C=O and N–H at 580–690 cm^{-1}. The characteristic absorption peaks of PPS are: stretching vibration of C=C in benzene at 1470 cm^{-1} and deformation vibration of =C–H in 1, 4 place of benzene at 818 cm^{-1}. It can be seen from Fig. 3 that the characteristic absorption peaks which are found in the PA66 and PPS spectra also appear in that of the blend at the same locations. In addition, there are no new absorption peaks in the blend spectrum. These observations suggest that in polymer blends, PA66 and PPS only blend with each other mechanically and no new chemical bonds are created.

The phase morphologies of the blends are shown in Fig. 4. These SEM pictures clearly illustrate the two-phase structure of the blends. Furthermore, the phase morphologies of the blends are correlated closely to their composition. When the PA66 content is predominant in the system, it forms a continuous phase in which discrete PPS particles of average size 0.2 μm are dispersed (Fig. 4a). The situation for PPS is as the same as for PA66, but the average size of dispersed PA66 particles is about 0.1 μm (Fig. 4b).

3.2. Mechanical properties

The mechanical properties of PA66, PPS and blends are listed in Table 3. It can be seen that, in general, the mechanical properties initially increase with PPS proportion, but gradually decrease later. Maximum values were obtained at PA66/PPS (70/30) for tensile, flexural and impact strengths, but for hardness at PA66/PPS (30/70). Based on these data, the best mechanical properties of materials were obtained for the PA66/PPS (70/30) blend.

Table 3
The mechanical properties of PA66/PPS blends

PA66/PPS blends	100/0	80/20	70/30	60/40	30/70	0/100
Tensile strength (MPa)	74.4	80.0	80.0	77.5	51.7	62.0
Flexural strength (MPa)	84.1	105	109	107	103	116
Impact strength (kJ/m^2)	2.0	3.9	4.9	3.0	2.4	3.2
Rockwell hardness (HRM)	82.2	84.2	90.3	90.7	92.8	86.0

3.3. Wear and friction

The curves showing the variation of friction coefficient with sliding time are given in Fig. 5. For almost all polymers, the friction coefficient rapidly increases in the early stage of sliding and reaches a steady value after 50 min. The tendency for the variation in friction coefficient of PA66 and PA66/PPS blends is about the same, but the friction coefficient of PPS is considerably higher than that of PA66 and PA66/PPS blends in the steady state.

A histogram of average friction coefficient and wear volume with PPS content is presented in Fig. 6. It was found that the differences in friction coefficient between PA66 and the other blends are not apparent (both about 0.66–0.68), but the friction coefficient of PPS is much higher (0.85). The wear volume of blends increases as the PPS percentage increases after its content exceeds 20 vol.%, below which the reverse trend is shown. The smallest wear volume is 4.99 mm^3 when PA66/PPS is 80/20, which is reduced by 25 and 90%, respectively, compared to the PA66 (6.71 mm^3) and PPS (46.4 mm^3), i.e. PA66/PPS (70/30) blend observably improves the wear resistance of PA66 and PPS.

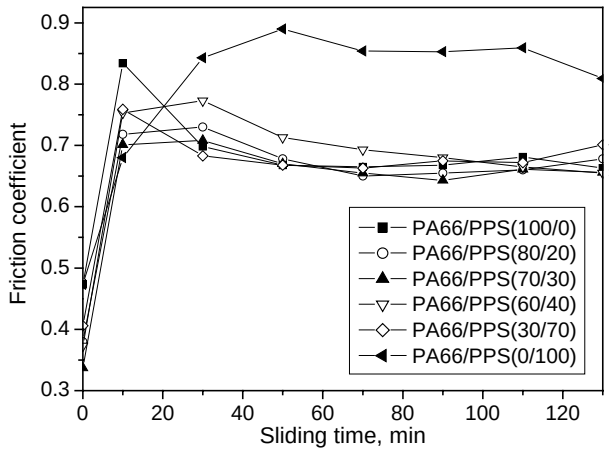

Fig. 5. Variation of friction coefficient with sliding time for PA66, PPS and their blends.

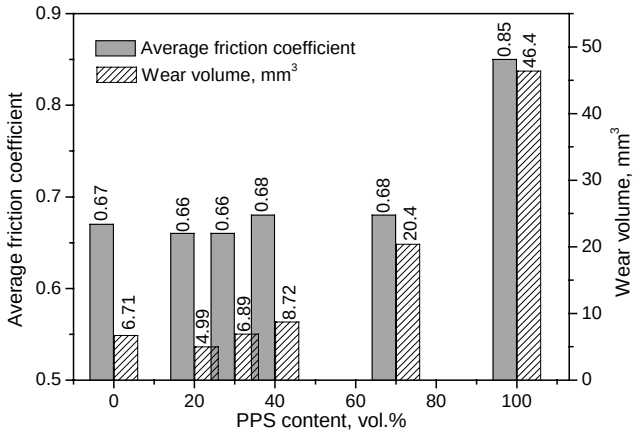

Fig. 6. Variation in average friction coefficient and wear volume with PPS content.

3.3.1. Analysis of wear debris

Analysis of wear debris is one of the powerful methods in the research of polymer tribology [21,22]. In order to elucidate the friction and wear mechanisms of polymer blends, the wear debris of PA66, PPS and their blends were analyzed by FT-IR and DSC.

The infrared spectra of PA66 and its debris are presented in Fig. 7. It was found that the peak positions were not changed before and after sliding. For example, four characteristic absorption bands of the amide group in polyamide (1636, 1539, 1270 and 580–690 cm^{-1}) and the stretching vibrations of methylene in the main chain (2926 and 2856 cm^{-1}) did not shift. However, for the characteristic absorption bands of amide groups, the peak intensities of the stretching vibration of C–N at 1270 cm^{-1} and the deformation vibration of N–H at 688 cm^{-1} decrease significantly in the wear debris. This may be due to the tribological change in PA66 because of frictional heat and a strong frictional shear force at the sliding interface.

The intensity, shape and position of absorption peaks in the fingerprint region of the FT-IR spectrum reflect the crystalline structure and type for a crystalline polymer [23]. Comparing the spectra of PA66 debris with that of pure PA66 in the fingerprint region, we can see that the position of each peak is very clear, the peak intensity is strong and the shape is acute for the latter, while for the former the peak intensity is weaker (especially for the absorption peaks at 1040 and 934 cm^{-1}), the peak shape is wider and many overlapping peaks appear. This indicates that during sliding, the original regular arrangement of the crystalline regions in PA66 is destroyed and the crystallinity dramatically decreases.

Analysis results for PPS and its debris are presented in Fig. 8. It can be seen that the peak positions of both PPS and its debris do not change and the peak intensity is nearly the same. This indicates that there are no tribochemical reactions during PPS sliding.

The FT-IR spectra of PA66/PPS (70/30) blend before and after tests are shown in Fig. 9. It can be seen that, compared with unworn blend, no changes occurred in the positions and intensities of characteristic absorption peaks for PPS (e.g. the peaks at 1470 and 818 cm^{-1}). Also there are no PA66 characteristic absorption peaks, or if there are some absorption peaks like those mentioned above, their intensities are very low. Absorption peaks at positions such as 1270, 933 and 688 cm^{-1} are changed typically. All of this indicates that the tribochemical reactions occurred in the PA66 phase during sliding, which was not the case for the PPS phase.

The DSC curves of debris for PA66, PPS and PA66/PPS (70/30) blend are given in Fig. 10. Compared with the DSC traces of respective samples before sliding (Fig. 2), there are no melting peaks in the debris traces and the shapes of the curves differ completely after sliding. This indicates that

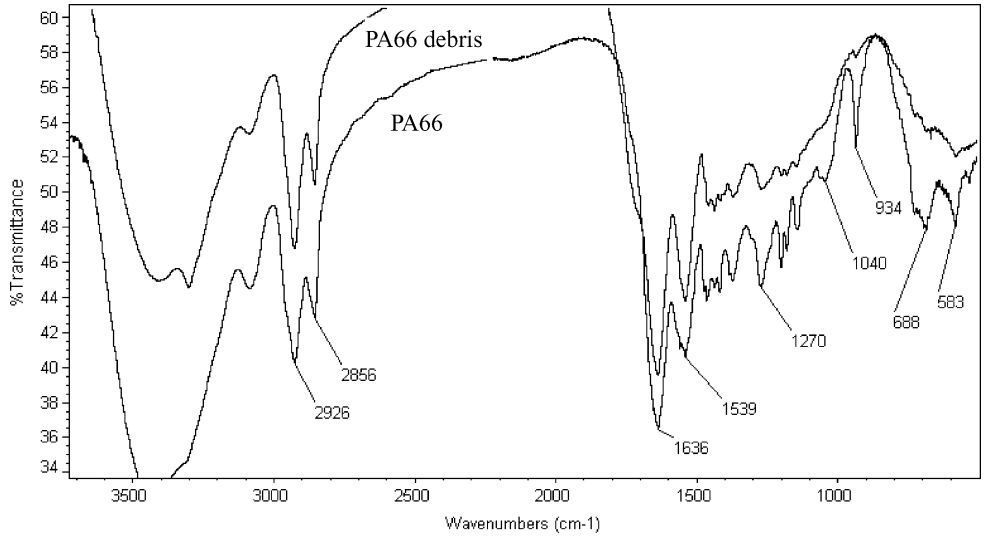

Fig. 7. The FT-IR spectra of PA66 and its debris.

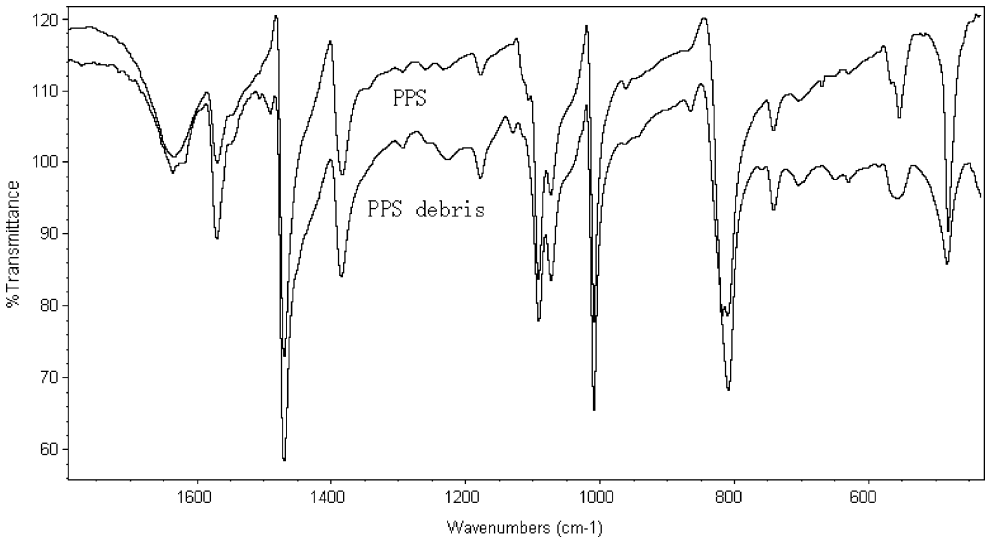

Fig. 8. The FT-IR spectra of PPS and its debris.

the crystalline structures of PA66, PPS and PA66/PPS blend were destroyed during sliding and the crystalline polymers changed into amorphous state.

3.3.2. Analysis of transfer films

It is now fully recognized that the friction and wear behavior of a polymer sliding against a metal counterface is strongly influenced by its ability to form a transfer film on the counterface. Because of this, the surfaces of steel rings sliding against polymers were investigated by SEM and EDS and the micrographs are given in Figs. 11–15.

The SEM micrograph of transfer film formed by PA66 and X-ray mapping of the elements are given in Fig. 11. Fig. 11a shows that PA66 forms a non-uniform and discontinuous transfer film on the surface of the steel ring. After cleaning the steel ring ultrasonically in acetone, the surface did not changed, which indicates a good adhesion between the transfer film and substrate. The transfer film consists of two portions: the dark portions and the bright portions. From the C-map (Fig. 11b) and Fe-map (Fig. 11c) in the transfer film it may be inferred that the dark portions are C enrichment regions, which indicate transfer of PA66 to the steel counterface. In contrast, carbon is almost not detected in the bright portions representing mostly Fe. Thus, the bright regions are the bare steel surfaces and have not been covered by the transfer film. A close examination of the O-map (Fig. 11d) shows its distribution is uniform and covering all the regions of the transfer film. This indicates the tribochemical reactions between the O_2 and Fe on the steel surface and transferred polymer under tribological heat and strong shear force during sliding, which facilitate adhesion between the transfer film and the counterface [22,24].

The SEM micrographs of surface of steel ring sliding against PPS are presented in Fig. 12. From Fig. 12a it can be

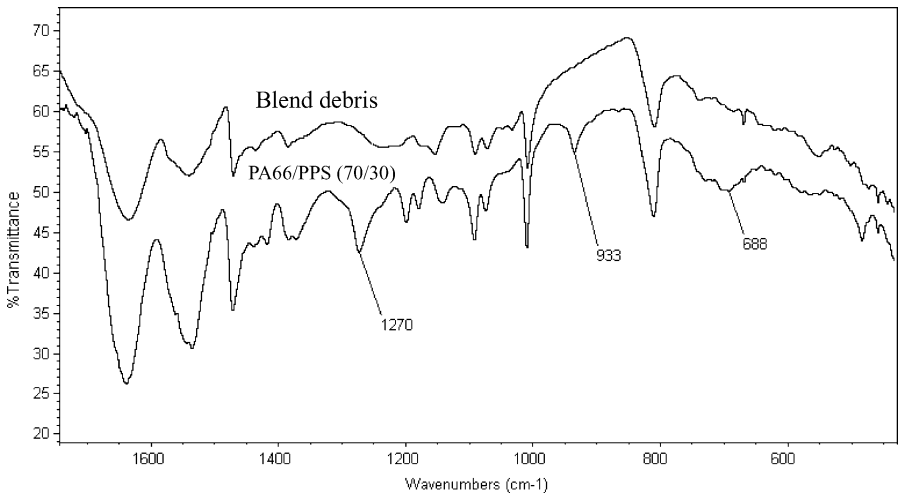

Fig. 9. The FT-IR spectra of PA66/PPS (70/30) blend and its debris.

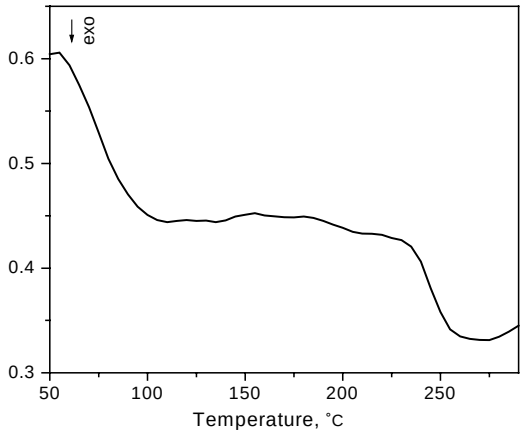

(a) PA66 debris.

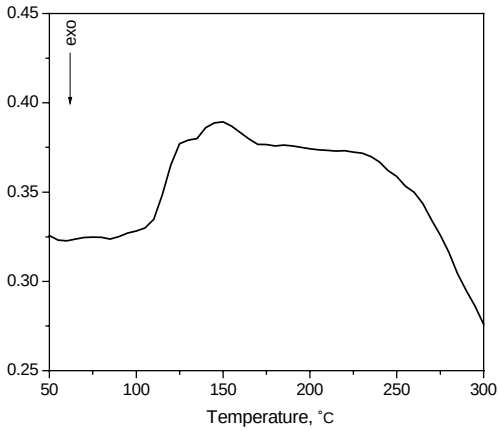

(b) PPS debris.

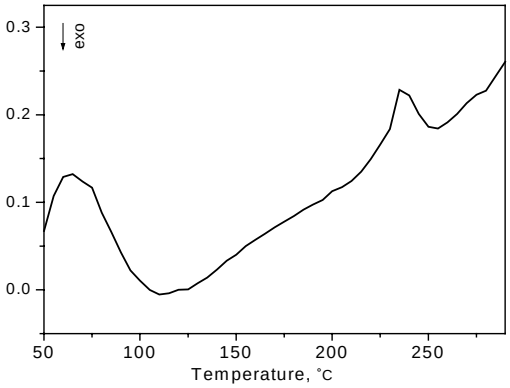

(c) Debris of PA66/PPS (70/30) blend.

Fig. 10. DSC traces of debris of PA66, PPS and PA66/PPS (70/30) blend.

seen that transferred PPS nearly did not cover the counterface, because the abrasion marks left by finishing the steel ring are clearly seen. The SEM micrograph at higher magnification (Fig. 12b) shows that the loose PPS particles were adsorbed on the surface. The particles were removed after cleaning the steel ring ultrasonically in acetone and sulfur element was almost not detected by EDS (as shown in Fig. 13). These results indicate that PPS has poor ability to form a transfer film on the steel counterface.

The SEM micrograph of transfer film formed by PA66/PPS (70/30) blend and X-ray mapping of the elements are given in Fig. 14. It also forms a non-uniform and discontinuous transfer film on the surface of the steel ring (Fig. 14a) and it did not changed after cleaning ultrasonically in acetone, which is similar to PA66. From Fig. 14b we can see that the oxygen distributes uniformly on the counterface. Relating with above discussion about transfer film of PA66, it can be inferred that the tribochemical reactions occurred with the PA66 phase for PA66/PPS blend. Comparing the C-map (Fig. 14c) with the S-map (Fig. 14d), it was found that there was abundant sulfur in the carbon enrichment regions, i.e. PPS in blend is also transferred to the steel counterface. This phenomenon, which is different from the pure PPS under the same conditions (PPS is unable to form an adhesive transfer film), indicates that the PA66 phase in the blends enhances the ability of PPS to form a transfer film on the counterface.

Fig. 15 shows the SEM micrographs of transfer film formed by PA66/PPS (30/70) blend before and after cleaning. Comparing Fig. 15(a) with Figs. 11(a) and 14(a), it was found that the coverage of transfer film increases with PPS content. However, the transfer film is rough and patch layers appeared on the surface. After cleaning ultrasonically in acetone, the patch layers were removed, which indicates that the adhesion between the transfer film and the substrate becomes weaker as PPS content increases in blends.

It has been hypothesized that wear resistance of polymers depends largely on their ability to form thin, uniform and adherent transfer film on the counterface [11,25–27]. The observations in this paper support the above hypothesis. The adhesive transfer film formed by PA66 during sliding prevents direct contact between the polymer surface and the hard counterface, thereby reducing abrasive action and resulting in lower wear volume. Since PPS has no ability to form an adhesive transfer film on the counterface, its wear depends on the mechanical interlocking between the con-

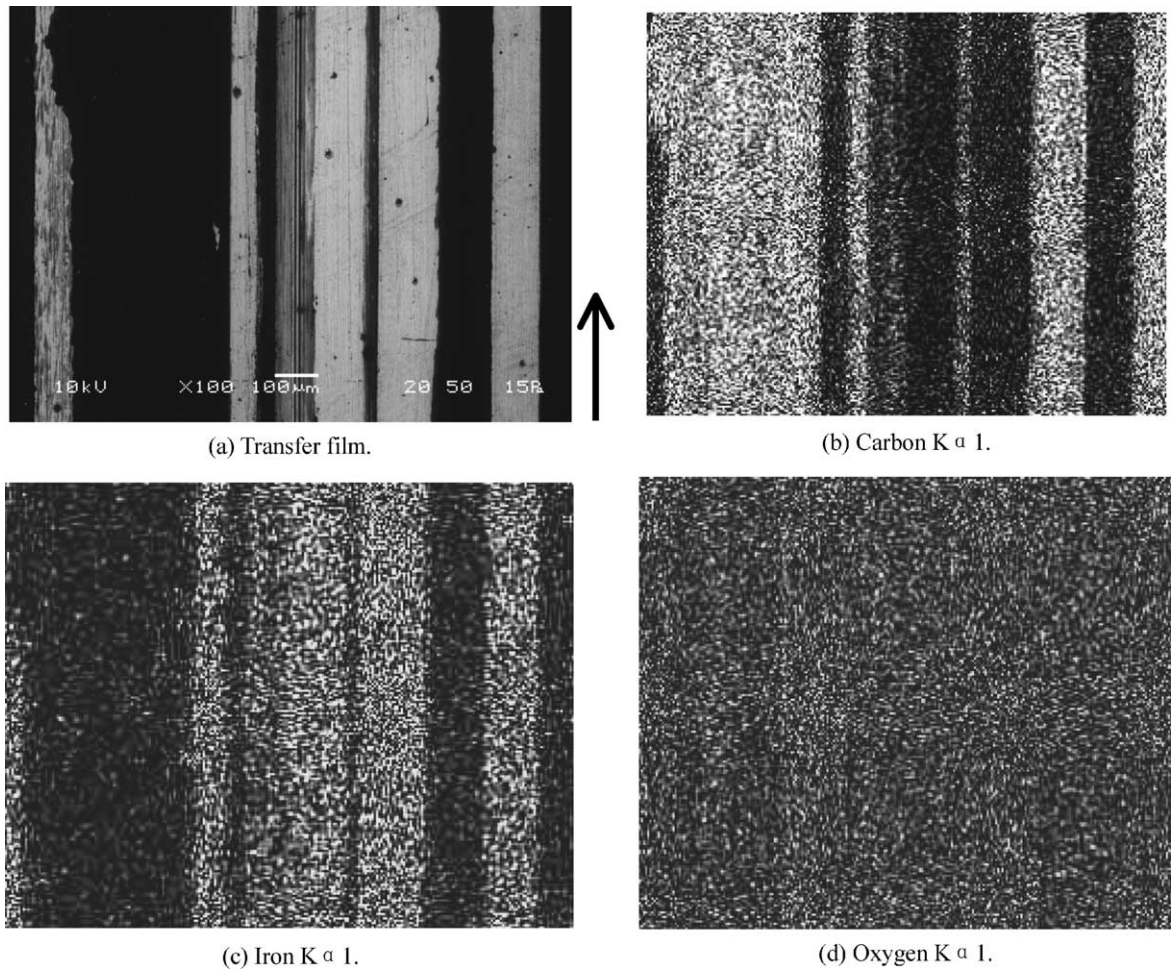

Fig. 11. SEM micrograph of transfer film formed by PA66 and X-ray mapping of the elements. Arrow indicates sliding direction.

tacting surfaces. During sliding, the hard asperities on the steel surface directly plow the surface of the polymer block because of the absence of adhesive transfer film. Polymer debris produced by plowing action are adsorbed mechanically on the counterface and are easily removed during sliding. Therefore, the wear volume of PPS is higher. As above mentioned, the PA66 phase in the blend enhances the ability of PPS to form a transfer film on the counterface, so the more PPS content, the larger amount of materials transferred to the counterface. However, because the

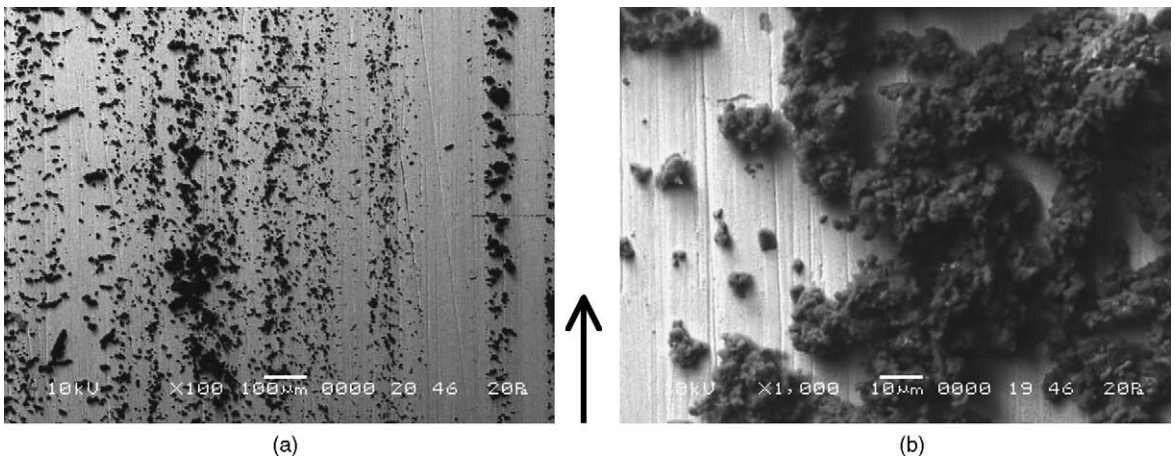

Fig. 12. SEM micrographs of counterface sliding against PPS. Arrow indicates sliding direction.

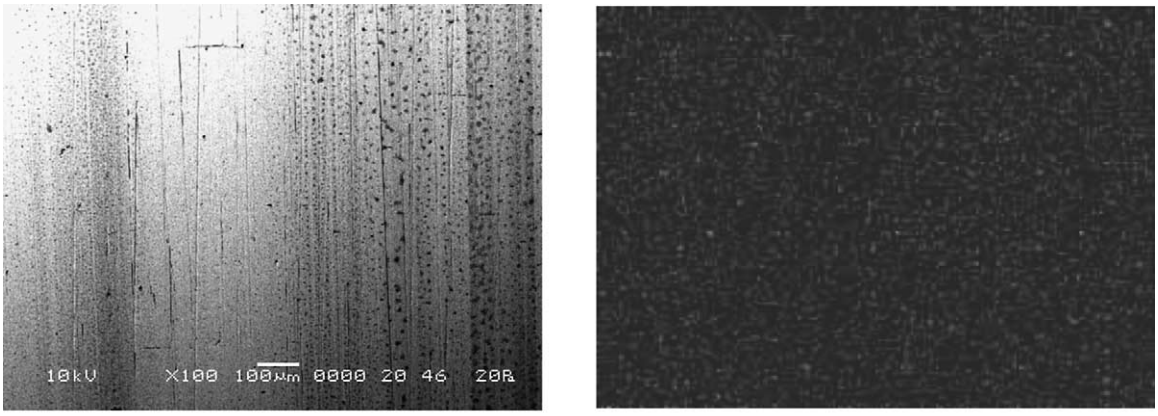

(a) Counterface. (b) Sulfur K α 1.

Fig. 13. SEM micrographs of counterface against PPS and S-map after cleaning.

adhesion between PPS and the substrate is very weak, so the transferred polymers on the counterface are easier to peel off. Therefore, the wear volume of the PA66/PPS blends increases with PPS content.

One experimental result to note in this paper is that a variation of friction coefficient for all blend compositions is about the same and it is also the same for pure PA66 (about 0.66–0.68, as shown in Fig. 6). We speculate that this can be explained by a thermal control of friction model [28,29]. In this model, frictional heat is not easily conducted from the interface because the low thermal conductivity of polymers. When sliding conditions are quite severe, a limiting condi-

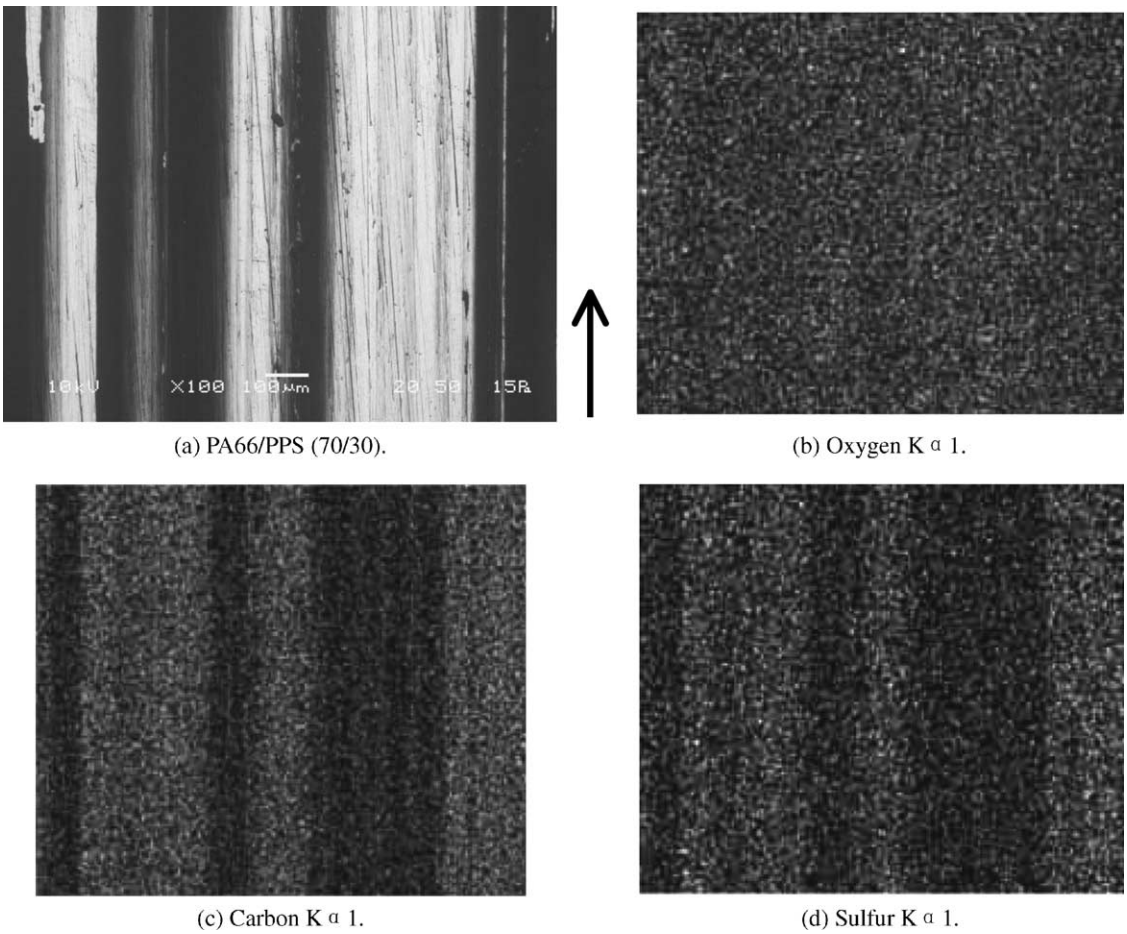

(a) PA66/PPS (70/30). (b) Oxygen K α 1.

(c) Carbon K α 1. (d) Sulfur K α 1.

Fig. 14. SEM micrograph of transfer film formed by PA66/PPS (70/30) blend and X-ray mapping of the elements. Arrow indicates sliding direction.

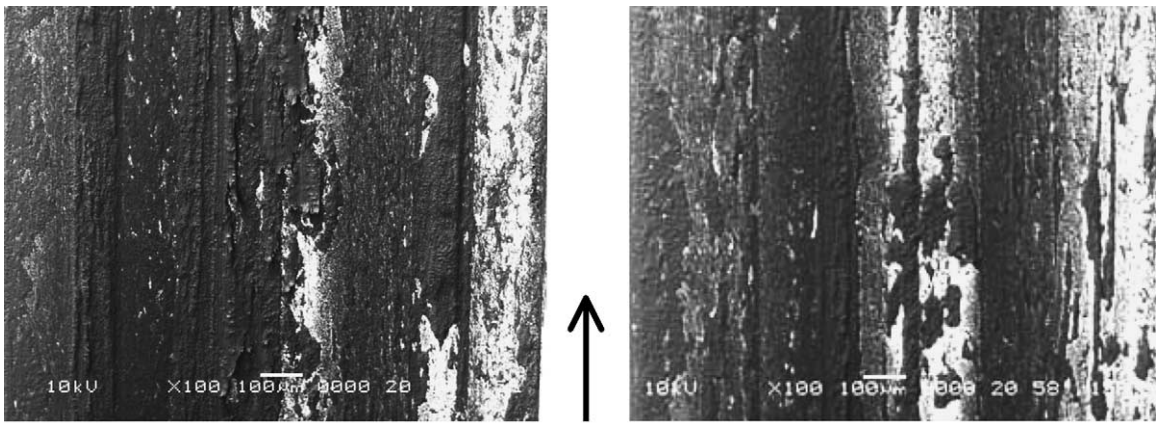

(a) Before cleaning. (b) After cleaning.

Fig. 15. SEM micrographs of transfer film formed by PA66/PPS (30/70) blend. Arrow indicates sliding direction.

tion will occur, beyond which frictional heating is actually the dominant factor. That is to say, when the melting temperature of the polymer is reached during sliding, the friction coefficient varies with sliding speed or load so that the temperature within the contact remains constant at the melting point. As for PA66/PPS blends used in this paper, which have a two-phase structure, the melting point of the PA66 phase (265 °C) is lower than that of the PPS phase (286 °C), so the melting point of PA66 is first reached and at that point the PA66 begins to melt. According to the thermal control of friction model, any additional frictional heat released in a contact during sliding tends to melt additional polymer rather than cause the temperature of the already molten polymer to rise. Thus, the temperature on the sliding surface did not

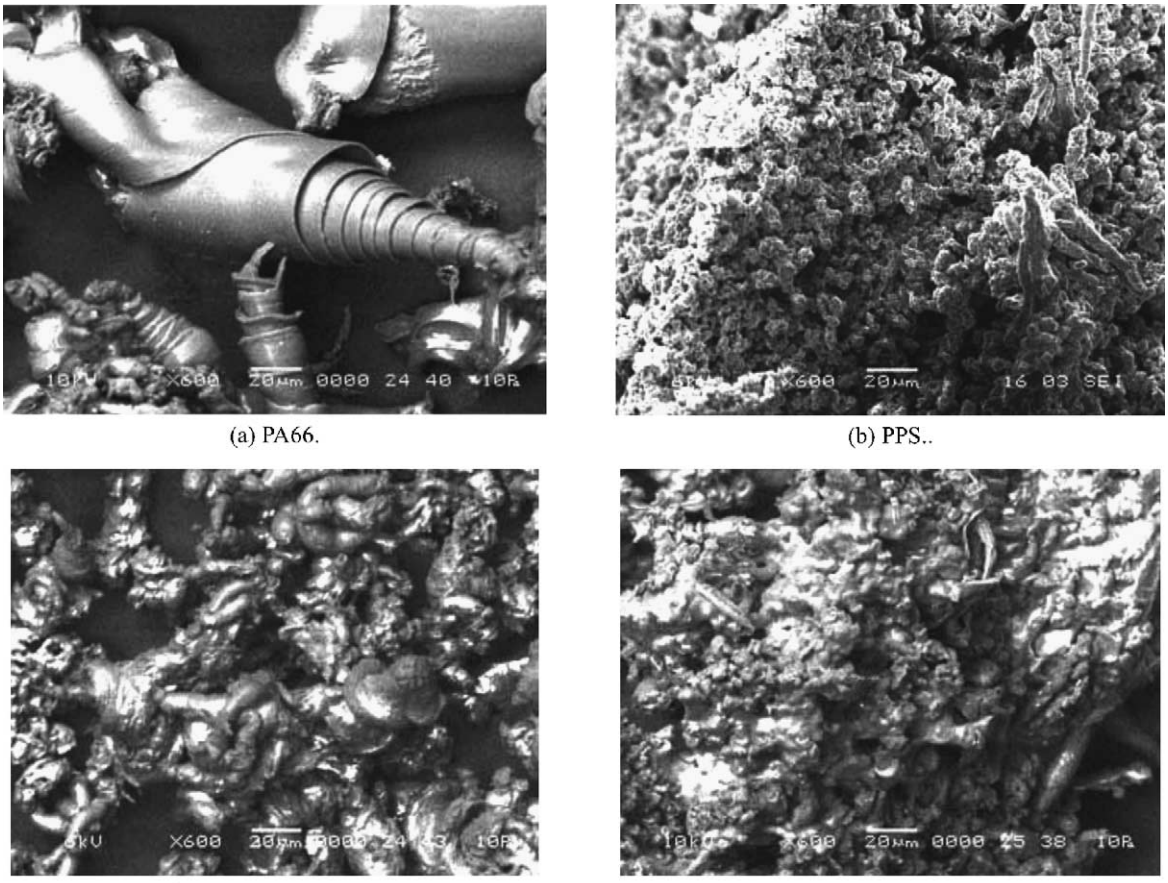

(a) PA66. (b) PPS..

(c) PA66/PPS (70/30). (d) PA66/PPS (30/70).

Fig. 16. The morphologies of wear debris formed by PA66, PPS and their blends.

increase when PA66 in the blends begins melting. Molten PA66 forms a low-shear-strength interfacial layer at the sliding surface, which behaves as a lubricant. In PA66 and blend systems, the friction coefficient is governed by the shear strength of this interfacial layer. For PA66/PPS blends showing a two-phase structure, the melting shear strength of the PA66 phase is equivalent to that of pure PA66, therefore, the differences in friction coefficient for PA66/PPS blends are not apparent and the values are nearly equal to that of pure PA66.

In order to prove above viewpoint, the morphologies of debris formed by PA66, PPS and PA66/PPS blends were investigated by SEM and the micrographs are given in Fig. 16. From this figure it can be seen that apparent melting phenomena occurred with PA66 and PA66/PPS blends, but PPS did not melt during sliding under the same conditions. Moreover, the melting intensity becomes weaker as the PPS content increases.

3.4. Remarks

The PA66/PPS blends improved the mechanical and tribological properties of the pure polymers. The mechanical properties are the best when the PA66/PPS ratio is 70/30. The friction coefficients of blends are nearly the same and approximately equal to that of pure PA66. The lowest wear volume (4.9 mm^3) is obtained with the PA66/PPS (80/20) blend. The PA66/PPS (70/30) blend has the lower friction coefficient and its wear volume is not very high (6.89 mm^3), so if taking into account the mechanical properties of materials, this blend compares favorably with other materials for practical applications.

Since the PA66/PPS blends have a two-phase structure and each phase in the system maintains the same properties as their own bulk polymer, so the changes in chemistry and physics for blends occurred during sliding are equivalent to that of the pure PA66 and pure PPS under the same conditions. In other words, the friction and wear process of PA66/PPS blends consists of that of the PA66 phase and PPS phase in the system. The friction coefficient of the blends is governed by the PA66 melting properties under the action of the thermal control of friction, while the adhesion between the PPS and steel surface is the major factor influencing the wear. That is to say, the different phases determine the friction and wear properties of the polymer blends separately. This provides the possibility of predicting the tribological properties of polymer blends. Based on this, it may be possible to produce polymer blends with superior properties of friction and wear.

4. Conclusions

On the basis of the studies made, the following conclusions may be drawn:

(1) The PA66/PPS blends improved the mechanical properties and the blend with best general mechanical properties is PA66/PPS (70/30).
(2) The friction coefficients of the blends and of the pure PA66 are almost the same (0.66–0.68), and they are much lower than that of the pure PPS (0.85).
(3) The minimum wear (4.99 mm^3) was obtained in the case of PA66/PPS (80/20) blend, the wear volume of blends increases with PPS proportion after the PPS content exceeds 20 vol.%, below which the reverse trend is shown.
(4) A tribochemical reaction takes place for pure PA66 during sliding, while not happening for pure PPS. The crystalline structures of PA66, PPS and PA66/PPS blends changed from the crystalline into the amorphous.
(5) PA66 has the ability to form a transfer film on the steel surface while PPS has not; the presence of PA66 phase in the blend enhances the ability of PPS to form a transfer film on the counterfaces.
(6) The thermal control of friction model is applicable for polymer blend systems. The friction coefficient is determined by the melting properties of the PA66 phase in the blends, and the wear is governed by the adhesion between PPS and the counterface.

Acknowledgements

The funding for this work was provided under contract number 0204 from the Ministry of Education of PR China.

References

[1] Y. Yamaguchi, Tribology of Plastic Materials, Tribology Series, vol. 16, Elsevier, New York, 1990, pp. 143–155.
[2] J. Hanchi, N.S. Eiss, Tribological behavior of polyetheretherketone, a thermotropic liquid crystalline polymer and in situ composites based on their blends under dry sliding conditions at elevated temperatures, Wear 200 (1996) 105–121.
[3] M. Palabiyik, S. Bahadur, Mechanical and tribological properties of polyamide 6 and high density polyethylene polyblends with and without compatibilizer, Wear 246 (2000) 149–158.
[4] M. Palabiyik, S. Bahadur, Tribological studies of polyamide 6 and high-density polyethylene blends filled with PTFE and copper oxide and reinforced with short glass fibers, Wear 253 (2002) 369–376.
[5] H. Canshu, L. Jihong, W. Qixian, C. Yongrong, Studies on the thermal behavior of PPS/PA-66 blends, Polym. Mater. Sci. Eng. 12 (1996) 110–113 (in Chinese).
[6] H. Canshu, L. Jihong, Y. Zili, Y. Yonggang, W. Qixian, Study on the structures and properties of PPS/PA66 blends, Polym. Mater. Sci. Eng. 14 (1998) 75–77 (in Chinese).
[7] S. Akhtar, J.L. White, Phase morphology and mechanical properties of blends of poly(*p*-phenylene sulfide) and polyamides, Polym. Eng. Sci. 32 (1992) 690–698.
[8] M. Watanabe, M. Karasawa, K. Matsubara, The frictional properties of nylon, Wear 12 (1968) 185–191.
[9] M. Watanabe, H. Yamaguchi, The friction and wear properties of nylon, Wear 110 (1986) 379–388.
[10] J.W.M. Mens, A.W.J. de Gee, Friction and wear behavior of 18 polymers in contact with steel in environments of air and water, Wear 149 (1991) 255–268.

[11] S. Bahadur, D. Gong, The role of copper compounds as fillers in transfer film formation and wear of nylon, Wear 154 (1992) 207–223.
[12] Y.K. Chen, S.N. Kukureka, C.J. Hooke, M. Rao, Surface topography and wear mechanisms in polyamide 66 and its composites, J. Mater. Sci. 35 (2000) 1269–1281.
[13] S.N. Kukureka, C.J. Hooke, M. Rao, P. Liao, Y.K. Chen, The effect of fibre reinforcement on the friction and wear of polyamide 66 under dry rolling–sliding contact, Tribol. Int. 32 (1999) 107–116.
[14] A. Bolvari, S. Glenn, R. Janssen, C. Ellis, Wear and friction of aramid fiber and polytetra-fluoroethylene filled composites, Wear 203–204 (1997) 697–702.
[15] Y. Laigui, The study on fillers mechanisms and tribology of polymer composites, Ph.D. Thesis, Lanzhou Institute of Chemical Physics, China Academy of Science, 1997.
[16] Y. Laigui, S. Bahadur, An investigation of the transfer film characteristics and the tribological behaviors of polyphenylene sulfide composites in sliding against tool steel, Wear 214 (1998) 245–251.
[17] Q. Zhao, S. Bahadur, A study of the modification of the friction and wear behavior of polyphenylene sulfide by particulate Ag_2S and PbTe fillers, Wear 217 (1998) 62–72.
[18] C.J. Schwartz, S. Bahadur, The role of filler deformability, filler–polymer bonding and counterface material on the tribological behavior of PPS, Wear 251 (2001) 123–140.
[19] Y. Yamamoto, T. Takashima, Friction and wear of water lubricated PEEK and PPS sliding contacts, Wear 253 (2002) 820–826.
[20] F. Li, K.-A. Hu, J.-L. Li, B.-Y. Zhao, The friction and wear characteristics of nanometer ZnO filled polytetrafluoroethylene, Wear 249 (2002) 877–882.
[21] J.H. Byett, C. Allen, Dry sliding wear behavior of polyamide 66 and polycarbonate composites, Tribol. Int. 25 (1992) 237–246.
[22] G. Jintang, M. Shaolan, L. Jinzhu, F. Dapeng, Tribochemical effects of some polymers/stainless steel, Wear 212 (1997) 238–243.
[23] W. Zhengxi, The Analysis and Identification of IR Spectra for Polymers, Sichuan University Press, Chengdu, 1989, pp. 178–184 (in Chinese).
[24] A.I. Sviridyonok, V.A. Bely, V.A. Smurugov, V.G. Savkin, A study of transfer in frictional interaction of polymers, Wear 26 (1973) 301–308.
[25] S. Bahadur, D. Gong, The role of copper compounds as fillers in the transfer and wear behavior of polyetheretherketone, Wear 154 (1992) 151–165.
[26] S. Bahadur, D. Gong, The transfer and wear of nylon and CuS–nylon composites: filler proportion and counterface characteristics, Wear 1621 (64) (1993) 397–406.
[27] S. Bahadur, A. Kapoor, The effect of ZnF_2, ZnS and PbS fillers on the tribological behavior of nylon 11, Wear 155 (1992) 49–61.
[28] C.M. Mc C. Ettles, Polymer and elastomer friction in the thermal control regime, ASLE Trans. 30 (1986) 149–159.
[29] G.W. Stachowiak, A.W. Batchelor, Engineering Tribology, 2nd ed., Boston, 2001, pp. 626–633.